lncRNA DHFRL1-4 knockdown attenuates cerebral ischemia/reperfusion injury by upregulating the levels of angiogenesis-related genes

YU ZHOU, DEZHI HUANG, YANG CAI, MING WANG, WENJIA MA, ZHONGZHONG JIANG and MIN LIU

Department of Neurosurgery, The Second Xiangya Hospital, Central South University, Changsha, Hunan 410011, P.R. China

Received February 23, 2022; Accepted May 17, 2022

DOI: 10.3892/ijmm.2022.5164

Abstract. The present study aimed to investigate the effects of long non-coding (lncRNA) dihydrofolate reductase-like 1 (DHFRL1-4) on cerebral ischemia/reperfusion (I/R)-induced injury. For this purpose, mice injected with lentivirus with small interfering RNA targeting DHFRL1-4 or negative control siRNA were used to construct models of cerebral I/R injury. Following the establishment of the model, the infarct size, neurological deficit score, apoptosis and the expression levels of basic fibroblast growth factor (bFGF), vascular endothelial growth factor (VEGF), Wnt family member 3a (Wnt3a), glycogen synthase kinase-3β (GSK-3β) and phosphorylated GSK-3β were assessed. The expression of DHFRL1-4 was significantly upregulated in the I/R model. In the control and sham groups, the boundaries between the cortex and gray matter were clear, and no edema or necrosis were observed. The nerve cells were arranged orderly and evenly, and the cell membranes were intact with visible nucleus and nucleolus. In the model group however, the nerve fibers were slightly necrotic and swollen, and the number of nerve cells was reduced. In the mice injected with si-DHFRL1-4 lentivirus, the brain tissues exhibited less liquefaction and degeneration, as well as less edema. Compared with the control and sham groups, the model group had a significantly larger infarct area, a higher apoptotic rate, higher bFGF, VEGF, Wnt3a and GSK-3β expression levels and a greater neurological deficit score. However, the mice injected with si-DHFRL1-4 lentivirus exhibited a significantly reduced infarct area, a lower apoptotic rate, lower Wnt3a and GSK-3β expression levels, a lower neurological deficit score, and significantly upregulated bFGF and VEGF levels.

Correspondence to: Dr Min Liu, Department of Neurosurgery, The Second Xiangya Hospital, Central South University, 139 Renmin Middle Road, Changsha, Hunan 410011, P.R. China
E-mail: xy2liumin@126.com

Abbreviations: DHFRL1-4, dihydrofolate reductase-like 1; Wnt3a, Wnt family member 3a; GSK-3β, glycogen synthase kinase-3β; I/R, ischemia/reperfusion; lncRNA, long non-coding RNA; TTC, 2,3,5-triphenyltetrazolium chloride; DMCAO, distal middle cerebral artery occlusion; H&E, hematoxylin and eosin; TUNEL, terminal deoxynucleotidyl transferase (TdT) dUTP nick-end labeling; bFGF, basic fibroblast growth factor; VEGF, vascular endothelial growth factor; ESC, embryonic stem cell; iPSC, inducible pluripotent stem cell; MCAO, middle cerebral artery occlusion; RT-qPCR, reverse transcription-quantitative polymerase chain reaction; GAPDH, glyceraldehyde-3-phosphate dehydrogenase; RIPA, radioimmunoprecipitation assay; HRP, horseradish peroxidase; DAPI, 4',6-diamidino-2-phenylindole

Key words: linc-DHFRL1-4, cerebral ischemia/reperfusion injury, gene expression, apoptosis, angiogenesis, ischemic stroke

Introduction

Ischemic stroke occurs when a blood clot blocks or narrows an artery, leading to the obstruction of blood supply to the brain. As the third highest cause of mortality and the most common cause of invalidity in the Western world, stroke affects 15 million individuals annually worldwide; five million of these individuals do not survive, and the other five million are permanently challenged physically (1). Currently, treatment for ischemic stroke involves the restoration of the blood supply to the ischemic area as soon as possible following its occurrence in order to prevent the death of neurons, glial cells and vascular endothelial cells (2). As regards acute ischemic stroke, the only effective treatment involves the use of thrombolysis drugs, such as intravenous tissue plasminogen activator (3) and endovascular therapy within 3-4.5 h of symptom onset (4). Since the treatment window is narrow and there are various hemorrhagic complications (3,5), the use of endovascular therapy is often limited (6). Mechanical thrombectomy in selected patients with acute ischemic stroke has also been able to produce partial or complete arterial recanalization (4). In addition, various combinations of antiplatelet therapies have been considered for various mechanisms of ischemia (7,8). However, the development of effective strategies with which to restore the blood supply in the ischemic brain tissue continues to pose a major challenge for stroke treatment (9).

Over the past years, several strategies have been used in the treatment of ischemic diseases. These treatments aim to restore the function of neurons, astroglia and oligodendroglia due to cerebral artery occlusion. For example, embryonic stem cells (ESCs) derived from pre-implantation embryos have the ability of unlimited self-renewal and the potential to differentiate into virtually any cell type. Following implantation into the cortex with severe focal ischemia in mouse models, mouse ESCs have been shown to express the surface markers of neurons, astrocytes and oligodendrocytes, leading to an improved functional recovery (10). The intrastriatal transplantation of mouse ESC-derived neuron-like cells has also been shown to improve dopaminergic function in mice with focal ischemia (11) and to promote the functional recovery of injured tissues (12-14). In addition, inducible pluripotent stem cells (iPSCs) have been found to be able to effectively reduce the total infarct volume and to markedly improve the behavior of mice with cerebral ischemia induced by middle cerebral artery occlusion (MCAO) when transplanted with fibrin glue (15).

Long non-coding RNAs (lncRNAs) are endogenous molecules without protein-encoding capacity. There is increasing evidence to suggest that lncRNAs play critical roles in several aspects of ischemic stroke and may thus be used as therapeutic targets in ischemic stroke (16). Cerebral ischemia has been found to alter lncRNA transcriptomic profiles in the microvascular endothelium, leading to the up- and down-regulation of lncRNAs interacting with transcription factors, with a potential role in mediating endothelial cell responses to ischemic stimuli (17). A number of lncRNAs have been found to be associated with the severity and prognosis of ischemic stroke, and inflammation (18-20). For example, the levels of lncNEAT1 have been found to be elevated in cells following ischemia/reperfusion (I/R), inducing cell apoptosis and inflammation; the knockdown of lncNEAT1 has been found to reduce I/R-induced apoptosis (21). In addition, a recent study demonstrated that FOXD3 antisense RNA 1 (FOXD3-AS1) was upregulated in response to ischemic injury in cardiomyocytes (22). The knockdown of FOXD3-AS1 was shown to attenuate cerebral I/R injury by upregulating Bcl2-like 13 expression (23). These findings suggest that both cell and gene therapies may provide new opportunities with which to manage ischemic stroke (24).

Several lncRNAs were found to be significantly upregulated in patients with ischemic stroke, including dihydrofolate reductase-like 1 (DHFRL1-4), small nucleolar RNA host gene 15 (SNHG15) and FAM98A-3, and may thus be used as novel diagnostic markers and therapeutic targets for ischemic stroke (25,26). For example, the suppression of SNHG15 has been found to attenuate I/R injury in SH-SY5Y cells (27). The present study aimed to investigate the effects on and possible mechanisms of action of DHFRL1-4 in cerebral I/R injury in order to explore novel strategies for the treatment of ischemic stroke. For this purpose, DHFRL1-4 expression was examined in a model of I/R injury and was knocked down using small inferring (si)RNA to investigate the pathological consequences. The findings presented herein may provide a new avenue with which to alleviate cerebral I/R injury and may also facilitate the translation of gene therapy in ischemic stroke treatment.

Materials and methods

Animals. A total of 30 male mice (weighing 25-30 g) were purchased from Shanghai SLAC Laboratory Animal Co., Ltd., and were exposed to artificial light from 6.00 a.m. to 8.30 p.m. in rooms with a controlled humidity (50%) and temperature (22˚C) for 7 days before being used in the experiments. The animals were housed under pathogen-free conditions and were provided with *ad libitum* access to a constant pellet diet and water. The experiments were carried out on mice aged 7 and 10 weeks. Following the completion of experiments, the mice were euthanized by CO_2 asphyxiation at a flow rate of 20% chamber volume per min which was immediately followed by decapitation. All animal experiments and animal care were conducted in accordance with the protocols approved by the Institutional Animal Care and Use Committee of the Second Xiangya Hospital, Central South University, Changsha, China. All animal research was performed in accordance with the ARRIVE guidelines (28).

Reagents, antibodies and instruments. The terminal deoxynucleotidyl transferase (TdT) dUTP nick-end labeling (TUNEL) assay kit (cat. no. ab66110), antibodies against Wnt family member 3a (Wnt3a; cat. no. ab219412, 1/1,000), basic fibroblast growth factor (bFGF; cat. no. ab92337, 1/1,500), glycogen synthase kinase-3β (GSK-3β; cat. no. ab32391, 1/1,000), phosphorylated (p-)GSK-3β (cat. no. ab75745, 1/1,000), glyceraldehyde-3-phosphate dehydrogenase (GAPDH; cat. no. ab8245, 1/1,000) and horseradish peroxidase (HRP)-labeled goat anti rabbit IgG (cat no. ab205719, 1/2,000) were obtained from Abcam. Rabbit antibody against vascular endothelial growth factor (VEGF; cat. no. sc-7269, 1/1,000) was obtained from Santa Cruz Biotechnology, Inc.; the polyvinylidene fluoride (PVDF) membrane (cat. no. IPVH00010) was purchased from MilliporeSigma; the Novex™ ECL Chemiluminescent Substrate Reagent kit (cat. no. WP20005), TRIzol® reagent (cat. no. 15596026), the RevertAid First Strand cDNA Synthesis kit (cat. no. K1621), TaqMan Pre-Amp Master Mix (cat. no. 4391128) and Lipofectamine™ RNAiMAX Transfection Reagent (cat. no. 13778030) were all purchased from Themo Fisher Scientific, Inc.; the ultrasensitive chemiluminescence imaging system (Chemi Doc™ XRS+) and fluorescence quantitative PCR (CFX Connect™) instruments were obtained from Bio-Rad Laboratories, Inc.

Reverse transcription-quantitative polymerase chain reaction (RT-qPCR). Brain tissue obtained from the mice was homogenized using an electric homogenizer and the total RNA was extracted using TRIzol® reagent (Themo Fisher Scientific, Inc.) according to the supplier's protocols. cDNA was then reverse transcribed from 1 μg total RNA using the RevertAid First Strand cDNA Synthesis kit according to the manufacturer's instructions. The reverse transcription reactions were carried out under the following conditions: 42˚C for 60 min; 25˚C for 5 min; and 70˚C for 5 min. RT-DHFRL1-4 was quantified by PCR reactions carried out under the following cycling conditions: Denaturing for 10 min at 95˚C, followed by 18 cycles, each one consisting of 15 sec at 95˚C and 4 min at 60˚C, on a CFX Connect PCR system. The qPCR mixtures had a final volume of 20 μl and contained 1 μl of template

cDNA, 0.5 μl of each sense (5'-TTACCCAAATAAAGTATA) and antisense primer (5'-ATGGGTGTTGAGCTTGAA), 10 μl of TaqMan pre-amp master mix, and 8 μl of diethyl pyrocarbonate (DEPC)-treated water. β-actin was used as an internal control with (forward primer, 5'-GACGTTGACATCCGTAAA GACC; and reverse primer, 5'-CTAGGAGCCAGGGCAGTA ATCT. Each reaction was repeated for at least three times, independently. Relative mRNA levels were calculated using the $2^{-\Delta\Delta Ct}$ method (29).

Animal grouping. The mice were randomly divided into the control (no treatment, n=6), sham-operated (sham; subjected to a procedure similar to DMCAO, although the carotid arteries were not ligated with a nylon suture, n=6) and the I/R model (subjected to DMCAO and carotid artery ligation, n=18) group. The I/R model group was further divided into the si-NC (I/R model infected with si-NC RNA, n=6) and the si-DHFRL1-4 (I/R model infected with si-DHFRL1-4 RNA, n=6) groups.

Transfection. si-NC (5'-TUCUCUTGCTUGUCAUACUTT-3') and si-DHFRL1-4 (5'-CCUCCUGUCUUGUUCUACUTT-3') were obtained from Nanjing KeyGen Biotech Co., Ltd. to knockdown DHFRL1-4. Mice (n=6) were anesthetized with pentobarbital sodium (30 mg/kg, Roiland Dingchang Technology, Co., Ltd.) and fixed on a 69100 Rotational Digital Stereotaxic Instrument (RWD Life Science Co., Ltd.) to inject RNA. Before the injection, 50 μl lentivirus si-NC or si-DHFRL1-4 (10^9 units/ml) were mixed with an equal volume of Lipofectamine RNAiMAX transfection reagent according to the manufacturer's instructions and injected into the lateral ventricle (0.2 mm posterior to the bregma, 1.0 mm lateral to the midline and 1.5 mm below the brain surface) using a microinjector equipped with the stereotaxic instrument at an injection rate of 10 μl/min. After 24 h later, the mice were used to construct the model of I/R.

Cerebral I/R model. The cerebral I/R model was constructed as previously described (30). Briefly, the mice were placed on heating pads to maintain their core body temperature at 37˚C after being anesthetized with pentobarbital sodium (30 mg/kg) for the surgery. Distal MCAO (DMCAO) was used to generate focal cerebral ischemia. To perform DMCAO, a smooth incision was made along the middle line of the neck to bluntly separate the left sternocleidomastoid and cervical muscles and to expose the right common carotid artery. The blood vessels were pulled out to the trigeminal nerve to expose the carotid arteries. The right common carotid artery and the proximal end of external carotid artery were ligated. A small incision was made on the right common carotid artery at a distance of 1 cm from the trigeminal point and a silicon-coated nylon suture (cat. no. 602156PK5Re, Doccol Corporation) was inserted into the carotid artery to block the blood flow. The blood flow was monitored using a RFLSI III Laser Speckle Contrast Imaging System (RWD Life Science Co., Ltd.). After 2 h, the suture was withdrawn to restore the blood reperfusion for 24 h. Cefazolin antibiotics (25 mg/kg; MilliporeSigma) were subcutaneously administered immediately following surgery, and slow-release buprenorphine (1 mg/kg; ZooPharm) was subcutaneously administered 24 h following surgery. The mice in the sham-operated (sham) group were treated in an identical manner, except that DMCAO was not performed with a silicon-coated nylon suture.

At 24 h after reperfusion, the neurologic deficit was carefully scored by a neurologist (one of the authors, WM) who was blinded to the animal treatments according to a previously described method (31). Briefly, the mice were held up gently by the tail one meter above the floor and observed for forelimb flexion. The mice that extended both forelimbs toward the floor and had no other neurological deficit were assigned grade 0, mice with any amount of consistent forelimb flexion and no other abnormality were graded as 1. Mice with decreased resistance to lateral push without and with circling were graded as 2 and 3.

2,3,5-Triphenyltetrazolium chloride (TTC) staining. TTC staining was used to visualize the infarct area. On day 7, the mice were deeply anesthetized by an intraperitoneal injection of 200 μl of sodium pentobarbital and were transcardially perfused with ice-cold PBS with 0.1% diethylpyrocarbonate (MilliporeSigma) for 3 min. The sodium pentobarbital method was used only for extracting brain tissue for TTC staining, as this was milder procedure and the aim was to maintain the brain tissue unaltered for TTC staining. The mice were decapitated and the brains were frozen at -80˚C for 60 min to dissect the cerebellum, brain stem and olfactory bulb. The brain tissues were sliced using a matrix device (Zivic Instruments) into 2-mm-thick coronal sections. The sections were incubated in 2% (TTC; MilliporeSigma) solution in the dark at 37˚C for 15 min. During this period, the brain slices were turned round every 5 min. The TTC-stained brain sections were imaged using a digital camera (Sony HDR-PJ790, Sony Corporation) for infarct size analyses. The infarct areas were traced using ImageJ software (version 1.2.1, National Institutes of Health) as previously described (32).

Hematoxylin and eosin (H&E) staining. H&E staining was used to visualize tissue damage as previously described (33). Briefly, the brain tissues were dehydrated through an ethanol gradient from 70 to 100% and cleared with three changes of xylene (1 min for each change). The dehydrated tissues were embedded in paraffin, sectioned to a thickness of 20 μm, dewaxed in xylene overnight and subsequently passed through 3x10 min 99% ethanol and 2x10 min 96% ethanol and rehydrated. The sections were immersed in an aqueous hematoxylin solution (cat. no. H9627, MilliporeSigma) for 3 min at 25˚C, differentiated with hydrochloric acid for 15 sec, rinsed briefly and counterstained with eosin (cat. no. 318906, MilliporeSigma) for 3 min at 25˚C. After rinsing thoroughly in distilled water and dehydrated as described above, the slides were cleared with xylene, sealed and examined under a microscope (Olympus CX33, Olympus Corporation).

TUNEL assay. TUNEL assay was carried to examine apoptosis in the brain tissue as previously described (34). Briefly, paraffin-embedded tissue sections were baked at 65˚C for 2 h and rehydrated by passing an ethanol serial gradient and incubated in 1 μg/ml proteinase K (cat. no. 25530049, Thermo Fisher Scientific, Inc.) in a 10 mM Tris solution (7.5 μl of 20 μg/μl proteinase K in 150 ml 10 mM Tris, pH 7.4-8.0) at room temperature for 15 min. The slides were then rinsed

with 1X PBS three times and blot-dried. Subsequently, 100 μl TUNEL reaction mixture were applied to each slide and the slides were incubated at 37˚C in the dark for 1 h in a humid chamber according to the supplier's protocols. The slides were then washed three times with PBS, immersed in 100 mM Tris buffer (pH 8.2) at room temperature for 5 min, followed by the addition of 100 μl substrate solution and incubation in the dark at room temperature for 10 min. The nuclei were counterstained with 2-(4-amidinophenyl)-6-indolecarbamidine dihydrochloride (DAPI; cat. no. MBD0015, MilliporeSigma) at 25˚C for 1 h. The slides were with then sealed with quenching solution and observed under a fluorescence microscope (Olympus BX51, Olympus Corporation).

Western blot analysis. For 10 mg tissue, 300 μl ice-cold radioimmunoprecipitation assay (RIPA) buffer (MilliporeSigma) were added and the tissue was homogenized using an electric homogenizer and agitated for 2 h at 4˚C. The lysates were centrifuged at 16,000 x g for 20 min at 4˚C and the proteins in the supernatant were quantified using the BCA protein assay kit (Thermo Fisher Scientific, Inc.) according to manufacturer's instructions. After denaturing by boiling at 100˚C for 5 min, ~50 μg proteins were loaded onto a 12% sodium dodecyl sulfate polyacrylamide gel and separated by electrophoresis at a constant voltage of 50 V. The proteins were then transferred to PVDF membranes by electroblotting in an ice bath at a constant voltage of 24 V. The PVDF membranes were then blocked with 5% non-fat milk in 1X Tris-buffered saline with 0.1% Tween-20 (TBST) for 4 h at room temperature and incubated overnight with primary antibodies against VEGF, Wnt3a, bFGF, GSK3β, p-GSK3β and GAPDH at 4˚C. The membranes were washed six times with Tris-buffered saline buffer, then incubated in HRP-conjugated goat anti-rabbit IgG (H+L) solution at room temperature for 2 h. The membranes were washed six times with PBS at room temperature and immunoreactive bands were visualized using the Novex ECL chemiluminescent substrate reagent kit in the dark according to the supplier's protocols. To quantify the proteins, the gray values of the bands were analyzed using Quantity One (version 4.62) analysis software (General Electric).

Statistical analysis. All data are expressed as the mean ± standard error of the mean (SEM) and were obtained from at least three independent assays. One-way analysis of variance with Tukey's post hoc test was used to investigate the differences among the various groups. Non-parametric ordinal data obtained for the neurologic deficit scores were analyzed using the Kruskal-Wallis test followed by Dunn's post hoc tests. A value of $P<0.05$ was considered to indicate a statistically significant difference.

Results

DHFRL1-4 expression is upregulated after I/R modeling and downregulated after DHFRL1-4 knockdown. The present study first assessed the expression of DHFRL1-4 in brain tissue after I/R modeling. The RT-qPCR data revealed that the mRNA level of DHFRL1-4 was significantly upregulated following in the I/R model group as compared with the control and sham groups (Fig. 1). However, following the injection of si-DHFRL1-4, the mRNA level of DHFRL1-4 was significantly decreased, although it was still slightly higher (although not significantly) than that of the control and sham groups. On the other hand, si-NC and sham operation did not markedly affect the DHFRL1-4 mRNA level (Fig. 1).

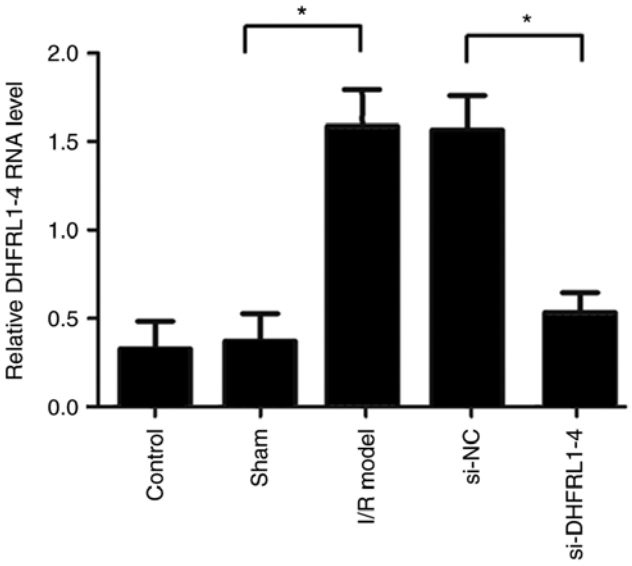

Figure 1. Relative mRNA level of DHFRL1-4 after I/R modeling and DHFRL1-4 knockdown in mouse brain tissue. *P<0.05. DHFRL1-4, dihydrofolate reductase-like 1; I/R, ischemia/reperfusion; si-DHFRL1-4, siRNA lentivirus targeting DHFRL1-4; si-NC, negative control siRNA.

DHFRL1-4 knockdown reduces the I/R-induced infarcted area and the neurologic deficit score. TTC staining revealed that following I/R modeling using the DMCAO procedure, the infarct area was significantly greater in the I/R group as compared to the control and sham groups, which di not exhibit an unstained area (Fig. 2). The injection of si-DHFRL1-4 before the I/R modelling significantly reduced the infarcted area as compared to the model group without the injection ($P<0.05$). On other hand, the injection of si-NC did not reduce the infarct area as compared to the model group. Similarly, I/R modelling significantly deteriorated nerve function, leading to higher neurological deficit scores in the I/R model group as compared to the control and sham groups (Fig. 2B); however, the knockdown of DHFRL1-4 significantly improved nerve function (Fig. 2B). Of note, no improvement was observed when si-NC was used ($P<0.05$; Fig. 2B).

DHFRL1-4 knockdown reduces the I/R-induced degeneration and necrosis of nerve cells. The present study then assessed brain tissue injury using H&E staining. The results revealed that in the control and sham groups, the cells were arranged in a regular manner, with a relatively uniform size and intact membranes. The nuclei and nucleoli were clear and visible (Fig. 3). In the model group however, some necrosis was observed in the nerve fibers, and the fibers were swollen and had edema. The number of nerve cells was less in the I/R model group, than that in the control and sham groups with large cell-cell gaps. However, following DHFRL1-4 knockdown, there was markedly less swelling and edema as compared to

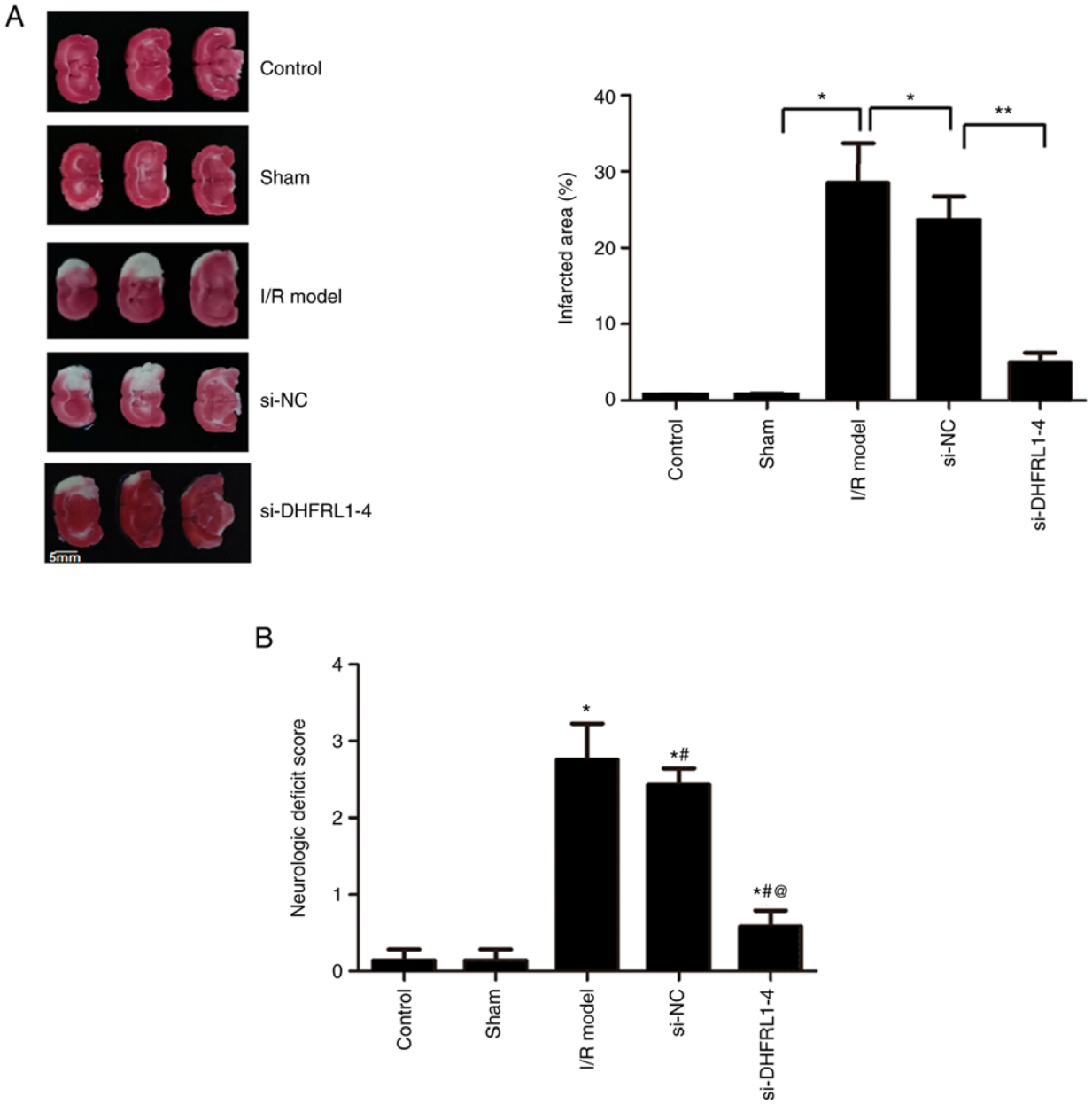

Figure 2. Cerebral infarct area and neurological deficit scores after I/R modeling and DHFRL1-4 knockdown in mice. (A) TTC staining of infarct area. Right panel, TTC staining results; left panel, infarct area. *P<0.05 and **P<0.01. (B) Neurological deficit score. *P<0.05, $^{\#}$P<0.05 and and $^{@}$P<0.05 compared to the sham, IR/model and si-NC groups, respectively. DHFRL1-4, dihydrofolate reductase-like 1; I/R, ischemia/reperfusion; si-DHFRL1-4, siRNA lentivirus targeting DHFRL1-4; si-NC, negative control siRNA; TTC, 2,3,5-triphenyltetrazolium chloride.

the model group; the brain tissue also exhibited less liquefaction and degeneration, and the distribution of nerve cells was relatively uniform (Fig. 3).

DHFRL1-4 knockdown reduces I/R-induced apoptosis. To further investigate the mechanisms underlying the reduction of I/R injury by the knockdown of DHFRL1-4, apoptosis in the brain tissue was assessed using TUNEL assay. Compared with the control and sham groups, there were significantly more apoptotic cells after I/R modelling (P<0.05). However, apoptosis was significantly reduced when the mice were injected with si-DHFRL1-4 before I/R modelling compared with the model group, although this was still higher than that in the control and sham groups (P<0.05). On the other hand, si-NC did not reduce apoptosis (P>0.05; Fig. 4).

DHFRL1-4 knockdown upregulates bFGF and VEGF expression. Since bFGF and VEGF are key growth factors related to angiogenesis, the expression of these two genes was examined in the brain tissue. Western blot analysis revealed that the expression levels of bFGF and VEGF were significantly increased after I/R modelling (P<0.05). DHFRL1-4 knockdown further upregulated these expression levels (P<0.05); however, si-NC did not alter bFGF and VEGF expression after I/R modelling (P>0.05; Fig. 5).

DHFRL1-4 knockdown downregulates Wnt3a and GSK-3β expression. In addition, western blot analysis revealed that the protein levels of Wnt3a, GSK-3β and p-GSK-3β were significantly upregulated after I/R modelling as compared with the control and sham groups (P<0.05 and P<0.01).

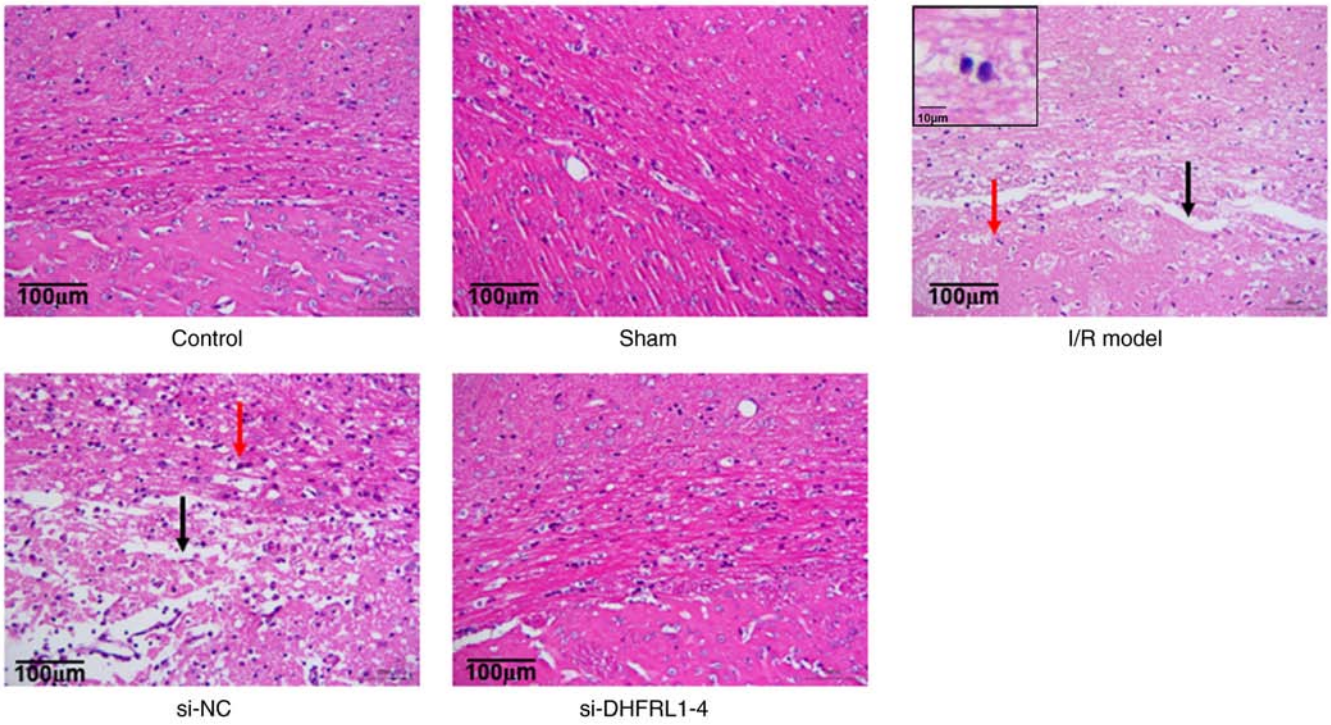

Figure 3. Hematoxylin and eosin staining of brain tissue after I/R modeling and DHFRL1-4 knockdown in mice. Black and red arrows indicate increased cell gaps (black arrows) and swollen nerve fibers (red arrows). The insert illustrates swollen nerve fibers as a result of I/R-induced damage at a higher magnification. DHFRL1-4, dihydrofolate reductase-like 1; I/R, ischemia/reperfusion; si-DHFRL1-4, siRNA lentivirus targeting DHFRL1-4; si-NC, negative control siRNA.

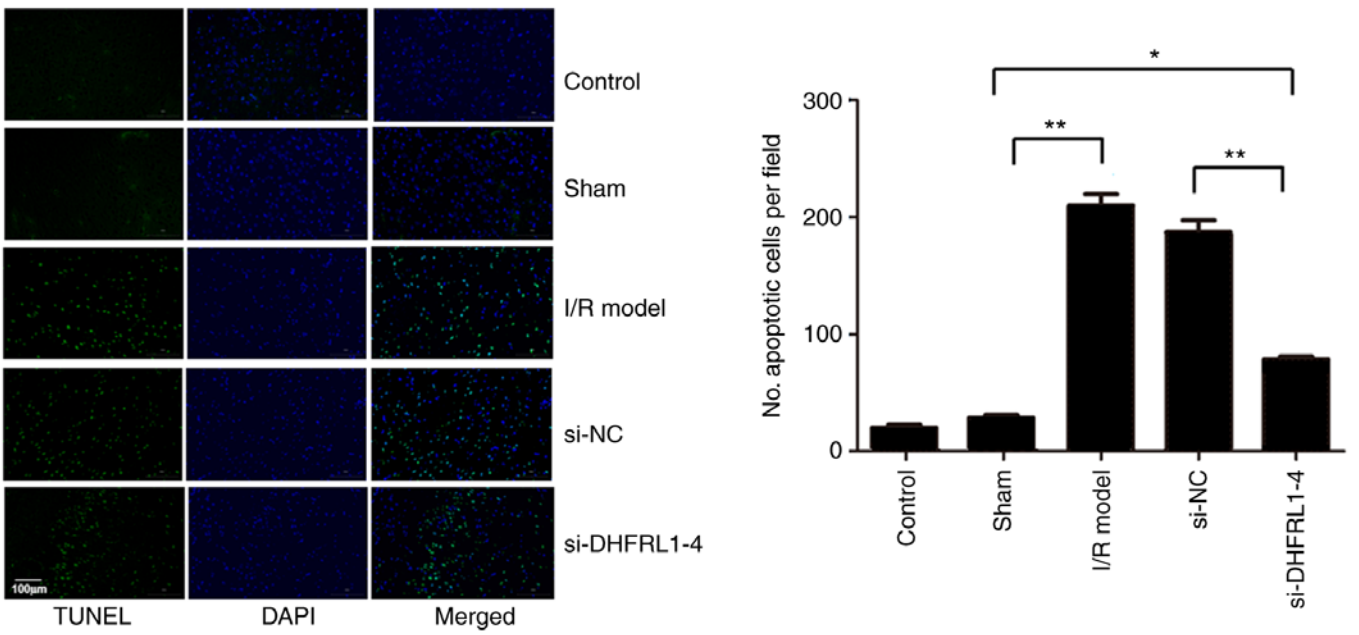

Figure 4. Assessment of apoptosis using TUNEL assay after I/R modeling and DHFRL1-4 knockdown in mice. Right panel, TUNEL assay images; left panel, apoptotic rates. *P<0.05 and **P<0.01. DHFRL1-4, dihydrofolate reductase-like 1; I/R, ischemia/reperfusion; si-DHFRL1-4, siRNA lentivirus targeting DHFRL1-4; si-NC, negative control siRNA; TUNEL, terminal deoxynucleotidyl transferase (TdT) dUTP nick-end labeling.

After DHFRL1-4 knockdown, the Wnt3a and GSK-3β levels were reduced; however, the p-GSK-3β level was not altered, resulting in an increased p-GSK-3β/GSK-3β ratio (P<0.01; Fig. 6). On the other hand, si-NC did not affect the protein levels compared with the I/R model group (P>0.05; Fig. 6).

Discussion

Despite recent advances being made in innovative treatment strategies, ischemic stroke remains one of the leading causes of mortality and disability worldwide. The present study attempted to explore whether lncRNAs can be used to

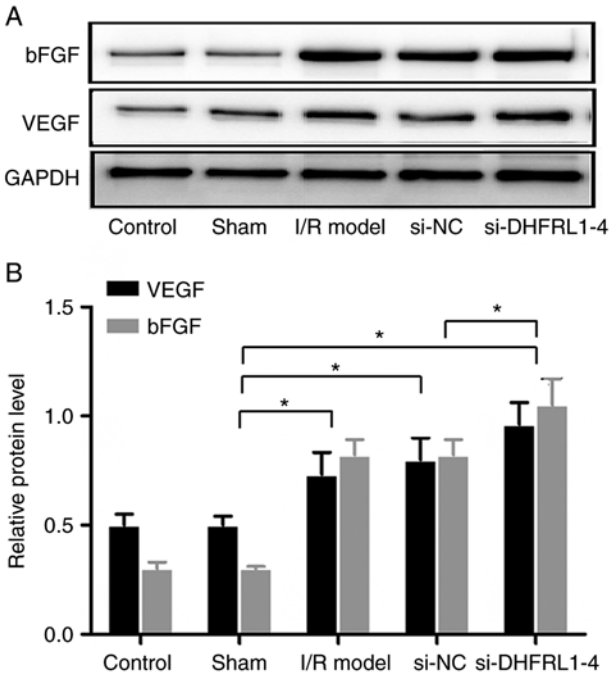

Figure 5. Expression of bFGF and VEGF after I/R modeling and DHFRL1-4 knockdown in mice. (A) Upper panel, representative western blots; (B) lower panel, relative protein levels. *P<0.05. DHFRL1-4, dihydrofolate reductase-like 1; I/R, ischemia/reperfusion; si-DHFRL1-4, siRNA lentivirus targeting DHFRL1-4; si-NC, negative control siRNA; bFGF, basic fibroblast growth factor; VEGF, vascular endothelial growth factor.

attenuate I/R-induced brain injury in a mouse model. It was found that the expression of DHFRL1-4 was upregulated in the model of I/R and DHFRL1-4 knockdown reduced I/R injury, degeneration and the necrosis of brain cells and apoptosis and improved neurological function. Molecular analysis revealed that following DHFRL1-4 knockdown, bFGF and VEGF expression levels were upregulated, and Wnt3a and GSK-3β expression levels were downregulated. These findings suggest that DHFRL1-4 may be further explored as a potential treatment target and avenue for ischemic stroke.

There is mounting evidence to indicate that lncRNAs play crucial roles in the occurrence and progression of solid tumors, atherosclerosis, blinding retinopathy and other diseases (35,36). A number of lncRNAs, including DHFRL1-4, have been found to be related the prognosis of ischemic stroke (18-20). Recent studies have demonstrated that several lncRNAs are upregulated in patients following ischemic stroke (25,26); however, whether the manipulation of lncRNA expression can be used to affect disease remains largely unclear. In the present study, it was found that following I/R, the expression of DHFRL1-4, which was upregulated in ischemic stroke patients (25), was significantly upregulated. This is in accordance with the findings of a previous study (25). Therefore, the present study attempted to knockdown the expression of DHFRL1-4 to examine its biological impact on I/R-induced injury using si-DHFRL1-4. The experimental data revealed that the DHFRL1-4 expression level was significantly decreased after the mice were injected with si-DHFRL1-4; however, it remained unaltered after the injection with si-NC, indicating that the knockdown was DHFRL1-4-specific. The examination of the infarct size revealed that there was significantly less injury after DHFRL1-4 knockdown with si-DHFRL1-4 as compared to the controls (si-NC), suggesting that the knockdown of DHFRL1-4 could attenuate I/R-induced injury. Furthermore, the neurological tests demonstrated that the mice injected with si-DHFRL1-4 behaved more normally as compared with the controls, suggesting that si-DHFRL1-4 could prevent damage to the nervous system. Cellular analysis revealed that I/R modelling resulted in the occurrence of necrosis and apoptosis in brain cells. However, in the mice injected with si-DHFRL1-4, there were significantly less necrotic cells and less apoptotic cells as compared with the control group. Taken together, these findings indicated that the knockdown of DHFRL1-4 significantly alleviated I/R-induced injury and may be further explored for ischemic stroke management.

Angiogenesis occurs within 4 to 7 days following cerebral ischemia in the border of the ischemic core and periphery. Therefore, it plays a crucial role in ischemic stroke and may facilitate functional recovery following ischemic stroke (37); thus, it may be one of the mechanisms underlying the observed protective role by DHFRL1-4 knockdown in the present study. The angiogensis of endothelial cells is regulated by a number of angiogenic genes, including bFGF (38) and VEGF (39,40). bFGF is one of the earliest, most extensively studied and most widely used fibroblast growth factors in the FGF family. It has potent angiogenesis-promoting activity. In the case of tissue injury, it can promote angiogenesis, provide nutrition for wound healing, and enhances the proliferation, migration and survival of endothelial cells (41,42). VEGF facilitates the proliferation and migration of endothelial cells after binding with kinase insert domain-containing receptor kinase in vascular endothelial cells (43,44). The present study demonstrated that the expression of bFGF and VEGF was significantly increased following I/R compared with the controls and was further upregulated following DHFRL1-4 knockdown; this suggests that one of the mechanisms underlying DHFRL1-4 mediated-protection may be associated with increased angiogenesis. However, the exact mechanisms through which DHFRL1-4 interacts with these angiogenesis-related factors remain to be elucidated.

A number signaling pathways have been implicated in I/R-induced injury and ischemic stroke, such as the PI3K/Akt pathway (45), the Notch signaling pathway (46) and the Wnt signaling pathway (47). The Wnt signaling pathway is a well-studied signaling pathway, which is involved in the proliferation, differentiation and axon formation of neural stem cells, and plays a critical role in cerebral vascular regeneration and remodeling (48). Previous research has demonstrated that Wnt/β-catenin signaling is involved in the mesenchymal stem cell-induced increase in the survival and neuronal differentiation of neuronal progenitor cells, and plays a main role in injury repair and neurovascular remodeling in ischemic stroke (49). It was also previously demonstrated that the Wnt signaling pathway was activated in rats when ischemic stroke occurred, leading to increased GSK-β phosphorylation (50,51). GSK-3β has been implicated in various diseases, including inflammation, neurodegenerative disease, diabetes and cancers, and is involved in several signal pathways, including the Wnt/β-catenin signaling pathway (52). The present study also found that the levels of Wnt3, GSK-β and p-GSK-β were

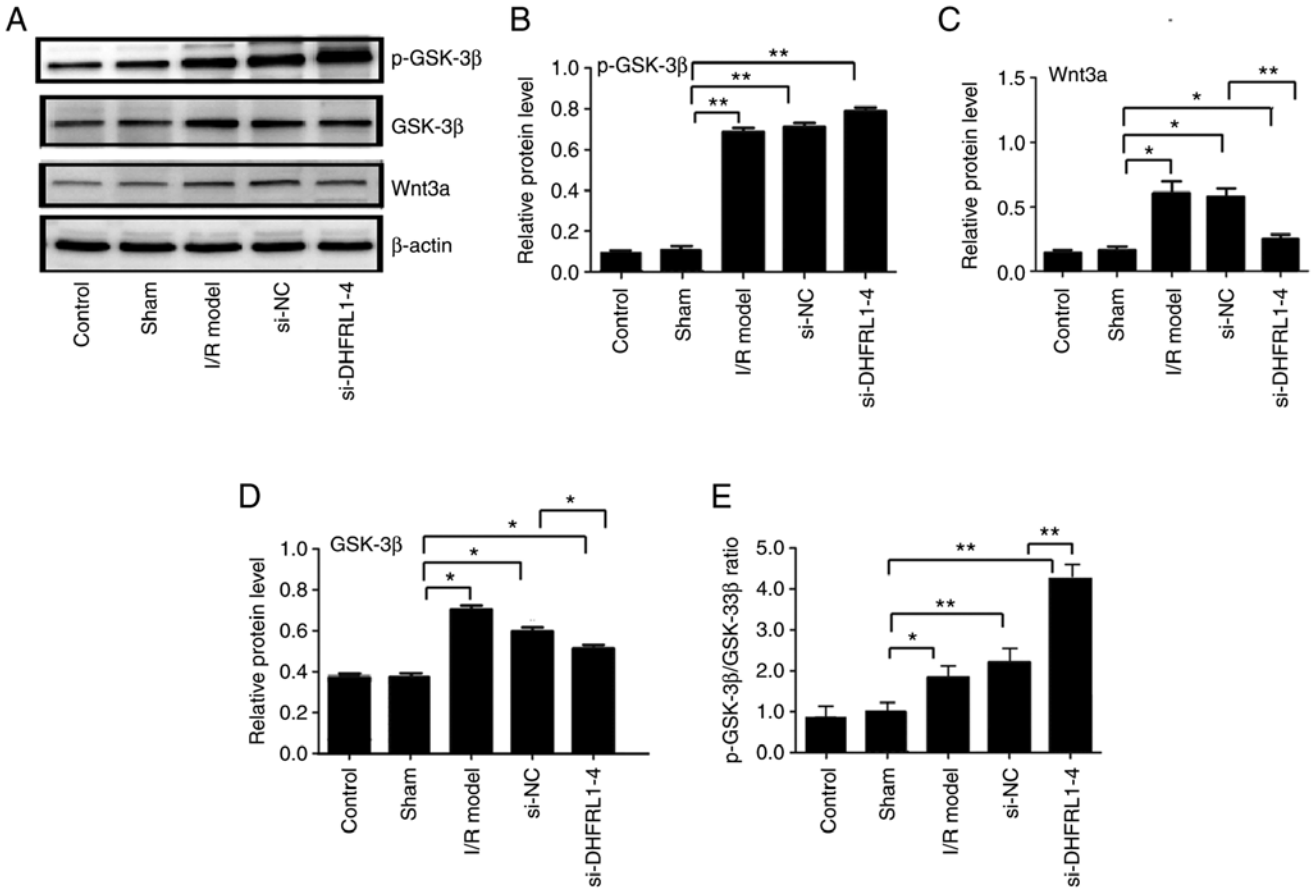

Figure 6. Expression of Wnt3a, GSK-3β and p-GSK-3β after I/R modeling and DHFRL1-4 knockdown in mice. (A) Representative western blots; (B-D) relative protein levels; (E) p-GSK3/GSK3 ratio. *P<0.05 and **P<0.01. DHFRL1-4, dihydrofolate reductase-like 1; I/R, ischemia/reperfusion; si-DHFRL1-4, siRNA lentivirus targeting DHFRL1-4; si-NC, negative control siRNA; Wnt3a, Wnt family member 3a; GSK-3β, glycogen synthase kinase-3β.

upregulated after I/R modelling. However, the levels of Wnt3 and GSK-β were downregulated following DHFRL1-4 knockdown, suggesting that DHFRL1-4 regulated the expression of the Wnt/β-catenin signaling pathway. In a previous study, the accumulation of p-GSK-β/GSK-β was observed in murine models of cerebral ischemia following treatment with tanshinol borneol ester, a synthetic therapeutic agent for ischemic stroke (53) and the activation of GSK3β/Nrf-2 signaling was associated with improved cerebral I/R-mediated injury (54). These results, however, are in contrast with the observations of the present study that Wnt3 and GSK-β expression levels were downregulated after DHFRL1-4 knockdown, in spite of improved I/R injury. Therefore, further studies are required to elucidate this discrepancy.

In the present study, it was found that VEGF, bFGF and pGSK were expressed in all treatment groups, including the controls. It is likely that these proteins have different levels of background expression and can be regulated by various biological and mechanical stimuli. For example, p-GSK is expressed in rat intestinal epithelial cells (55) and in an I/R model of ischemic stroke (56). As a potent stimulator of angiogenesis, VEGF is expressed in multiple cell types and its expression is regulated developmentally (57) and by a number of factors, such as metallothionein-III (58), osteoarthritis (59) and can also be upregulated by vascular damage and in wounds (60,61). bFGF is also expressed in non-wound tissue, and its expression can be upregulated during the wound healing process by treatment with collagen extract (62) and kefir (63), and even by surgical debridement (64). As a lncRNA, DHFRL1-4 may regulate the expression of these genes via its interaction with microRNAs, or serving as a scaffold for modifying protein complexes (65). It may also alter the chromatin conformation of spatially related genes to regulate their expression (66). However, the exact mechanisms through which DHFRL1-4 regulates the expression of VEGF, bFGF and pGSK remain to be investigated.

In conclusion, the present study demonstrated that DHFRL1-4 was upregulated in I/R-damaged brain tissue and DHFRL1-4 knockdown reduced I/R-induced apoptosis, and attenuated neurological deficits and the degeneration of brain cells. This attenuation may be partially attributed to the upregulation of angiogenesis-related genes and the downregulation of the Wnt signaling pathway, although specific underlying mechanisms remain to be elucidated.

Acknowledgements

Not applicable.

Funding

The present study was performed with the regular operation budget of the Department of Neurosurgery, the Second Xiangya Hospital, Central South University, Changsha, China.

Availability of data and materials

The datasets used and/or analyzed during the current study are available from the corresponding author on reasonable request.

Authors' contributions

YZ, DH and ML designed the study. YZ, DH, YC, MW, WM and ZJ performed the experiments. YZ, DH, YC, MW, WM, ZJ and ML collected the data and performed the analyses. YZ, DH, YC, MW, WM, ZJ and ML drafted the manuscript. YZ, DH and ML confirm the authenticity of all the raw data. All authors have read and approved the final version of manuscript.

Ethics approval and consent to participate

All animal experiment protocols were approved by the Institutional Animal Care and Use Committee of the Second Xiangya Hospital, Central South University, Changsha, China (approval no. 2020438).

Patient consent for publication

Not applicable.

Competing interests

The authors declare that they have no competing interests.

References

1. WHO publishes definitive atlas on global heart disease and stroke epidemic. Indian J Med Sci 58: 405-406, 2004.
2. Jena I, Nayak SR, Behera S, Singh B, Ray S, Jena D, Singh S and Sahoo SK: Evaluation of ischemia-modified albumin, oxidative stress, and antioxidant status in acute ischemic stroke patients. J Nat Sci Biol Med 8: 110-113, 2017.
3. National Institute of Neurological Disorders and Stroke rt-PA Stroke Study Group: Tissue plasminogen activator for acute ischemic stroke. N Engl J Med 333: 1581-1587, 1995.
4. Prabhakaran S, Ruff I and Bernstein RA: Acute stroke intervention: A systematic review. JAMA 313: 1451-1462, 2015.
5. Thomalla G, Sobesky J, Köhrmann M, Fiebach JB, Fiehler J, Zaro Weber O, Kruetzelmann A, Kucinski T, Rosenkranz M, Röther J and Schellinger PD: Two tales: Hemorrhagic transformation but not parenchymal hemorrhage after thrombolysis is related to severity and duration of ischemia: MRI study of acute stroke patients treated with intravenous tissue plasminogen activator within 6 h. Stroke 38: 313-318, 2007.
6. Yoshimura S, Sakai N, Uchida K, Yamagami H, Ezura M, Okada Y, Kitagawa K, Kimura K, Sasaki M, Tanahashi N, *et al*: Endovascular therapy in ischemic stroke with acute large-vessel occlusion: Recovery by endovascular salvage for cerebral ultra-acute embolism Japan registry 2. J Am Heart Assoc 7: e008796, 2018.
7. SPS3 Investigators, Benavente OR, Hart RG, McClure LA, Szychowski JM, Coffey CS and Pearce LA: Effects of clopidogrel added to aspirin in patients with recent lacunar stroke. N Engl J Med 367: 817-825, 2012.
8. Hong KS, Lee SH, Kim EG, Cho KH, Chang DI, Rha JH, Bae HJ, Lee KB, Kim DE, Park JM, *et al*: Recurrent ischemic lesions after acute atherothrombotic stroke: Clopidogrel plus aspirin versus aspirin alone. Stroke 47: 2323-2330, 2016.
9. Moussouttas M and Papamitsakis NIH: Critique on the use of early short-term dual antiplatelet therapy following minor acute cerebral ischemic events. Cerebrovasc Dis 49: 237-243, 2020.
10. Wei L, Cui L, Snider BJ, Rivkin M, Yu SS, Lee CS, Adams LD, Gottlieb DI, Johnson EM Jr, Yu SP and Choi DW: Transplantation of embryonic stem cells overexpressing Bcl-2 promotes functional recovery after transient cerebral ischemia. Neurobiol Dis 19: 183-193, 2005.
11. Yanagisawa D, Qi M, Kim DH, Kitamura Y, Inden M, Tsuchiya D, Takata K, Taniguchi T, Yoshimoto K, Shimohama S, *et al*: Improvement of focal ischemia-induced rat dopaminergic dysfunction by striatal transplantation of mouse embryonic stem cells. Neurosci Lett 407: 74-79, 2006.
12. Abdelwahid E, Siminiak T, Guarita-Souza LC, Teixeira de Carvalho KA, Gallo P, Shim W and Condorelli G: Stem cell therapy in heart diseases: A review of selected new perspectives, practical considerations and clinical applications. Curr Cardiol Rev 7: 201-212, 2011.
13. Gutiérrez-Fernández M, Rodríguez-Frutos B, Ramos-Cejudo J, Otero-Ortega L, Fuentes B and Díez-Tejedor E: Stem cells for brain repair and recovery after stroke. Expert Opin Biol Ther 13: 1479-1483, 2013.
14. Lee EJ, Park HW, Jeon HJ, Kim HS and Chang MS: Potentiated therapeutic angiogenesis by primed human mesenchymal stem cells in a mouse model of hindlimb ischemia. Regen Med 8: 283-293, 2013.
15. Chen SJ, Chang CM, Tsai SK, Chang YL, Chou SJ, Huang SS, Tai LK, Chen YC, Ku HH, Li HY and Chiou SH: Functional improvement of focal cerebral ischemia injury by subdural transplantation of induced pluripotent stem cells with fibrin glue. Stem Cells Dev 19: 1757-1767, 2010.
16. Wang Q, Liu X and Zhu R: Long noncoding RNAs as diagnostic and therapeutic targets for ischemic stroke. Curr Pharm Des 25: 1115-1121, 2019.
17. Zhang J, Yuan L, Zhang X, Hamblin MH, Zhu T, Meng F, Li Y, Chen YE and Yin KJ: Altered long non-coding RNA transcriptomic profiles in brain microvascular endothelium after cerebral ischemia. Exp Neurol 277: 162-170, 2016.
18. Ren H, Wu F, Liu B, Song Z and Qu D: Association of circulating long non-coding RNA MALAT1 in diagnosis, disease surveillance, and prognosis of acute ischemic stroke. Braz J Med Biol Res 53: e9174, 2020.
19. Na L, Ding H, Xing E, Gao J, Liu B, Wang H, Yu J and Yu C: Lnc-MEG3 acts as a potential biomarker for predicting increased disease risk, systemic inflammation, disease severity, and poor prognosis of sepsis via interacting with miR-21. J Clin Lab Anal 34: e23123, 2020.
20. Zhang Y and Niu C: The correlation of long non-coding RNA intersectin 1-2 with disease risk, disease severity, inflammation, and prognosis of acute ischemic stroke. J Clin Lab Anal 34: e23053, 2020.
21. Wang L, Qu P, Yin W and Sun J: Lnc-NEAT1 induces cell apoptosis and inflammation but inhibits proliferation in a cellular model of hepatic ischemia/reperfusion injury. J Int Med Res 49: 300060519887251, 2021.
22. Tong G, Wang Y, Xu C, Xu Y, Ye X, Zhou L, Zhu G, Zhou Z and Huang J: Long non-coding RNA FOXD3-AS1 aggravates ischemia/reperfusion injury of cardiomyocytes through promoting autophagy. Am J Transl Res 11: 5634-5644, 2019.
23. Lu Y, Han Y, He J, Zhou B, Fang P and Li X: LncRNA FOXD3-AS1 knockdown protects against cerebral ischemia/reperfusion injury via miR-765/BCL2L13 axis. Biomed Pharmacother 132: 110778, 2020.
24. Yamashita T, Deguchi K, Nagotani S, Kamiya T and Abe K: Gene and stem cell therapy in ischemic stroke. Cell Transplant 18: 999-1002, 2009.
25. Deng QW, Li S, Wang H, Sun HL, Zuo L, Gu ZT, Lu G, Sun CZ, Zhang HQ and Yan FL: Differential long noncoding RNA expressions in peripheral blood mononuclear cells for detection of acute ischemic stroke. Clin Sci (Lond) 132: 1597-1614, 2018.
26. Montaner J, Ramiro L, Simats A, Tiedt S, Makris K, Jickling GC, Debette S, Sanchez JC and Bustamante A: Multilevel omics for the discovery of biomarkers and therapeutic targets for stroke. Nat Rev Neurol 16: 247-264, 2020.
27. Wen Y, Zhang X, Liu X, Huo Y, Gao Y and Yang Y: Suppression of lncRNA SNHG15 protects against cerebral ischemia-reperfusion injury by targeting miR-183-5p/FOXO1 axis. Am J Transl Res 12: 6250-6263, 2020.
28. Kilkenny C, Browne WJ, Cuthill I, Emerson M and Altman DG: Improving bioscience research reporting: The ARRIVE guidelines for reporting animal research. PLoS Biol 8: e1000412, 2010.
29. Livak KJ and Schmittgen TD: Analysis of relative gene expression data using real-time quantitative PCR and the 2(-Delta Delta C(T)) method. Methods 25: 402-408, 2001.
30. Doyle KP, Fathali N, Siddiqui MR and Buckwalter MS: Distal hypoxic stroke: A new mouse model of stroke with high throughput, low variability and a quantifiable functional deficit. J Neurosci Methods 207: 31-40, 2012.

31. Bederson JB, Pitts LH, Tsuji M, Nishimura MC, Davis RL and Bartkowski H: Rat middle cerebral artery occlusion: Evaluation of the model and development of a neurologic examination. Stroke 17: 472-476, 1986.
32. Murtha LA, Beard DJ, Bourke JT, Pepperall D, McLeod DD and Spratt NJ: Intracranial pressure elevation 24 h after ischemic stroke in aged rats is prevented by early, short hypothermia treatment. Front Aging Neurosci 8: 124, 2016.
33. Fischer AH, Jacobson KA, Rose J and Zeller R: Hematoxylin and eosin staining of tissue and cell sections. CSH Protoc 2008: pdb.prot4986, 2008.
34. Kyrylkova K, Kyryachenko S, Leid M and Kioussi C: Detection of apoptosis by TUNEL assay. Methods Mol Biol 887: 41-47, 2012.
35. Zhao Z, Sun W, Guo Z, Zhang J, Yu H and Liu B: Mechanisms of lncRNA/microRNA interactions in angiogenesis. Life Sci 254: 116900, 2020.
36. Beermann J, Piccoli MT, Viereck J and Thum T: Non-coding RNAs in development and disease: Background, mechanisms, and therapeutic approaches. Physiol Rev 96: 1297-1325, 2016.
37. Hatakeyama M, Ninomiya I and Kanazawa M: Angiogenesis and neuronal remodeling after ischemic stroke. Neural Regen Res 15: 16-19, 2020.
38. Wilkins JR, Pike DB, Gibson CC, Kubota A and Shiu YT: Differential effects of cyclic stretch on bFGF- and VEGF-induced sprouting angiogenesis. Biotechnol Prog 30: 879-888, 2014.
39. Shima DT, Gougos A, Miller JW, Tolentino M, Robinson G, Adamis AP and D'Amore PA: Cloning and mRNA expression of vascular endothelial growth factor in ischemic retinas of Macaca fascicularis. Invest Ophthalmol Vis Sci 37: 1334-1340, 1996.
40. Cantaluppi V, Biancone L, Figliolini F, Beltramo S, Medica D, Deregibus MC, Galimi F, Romagnoli R, Salizzoni M, Tetta C, *et al*: Microvesicles derived from endothelial progenitor cells enhance neoangiogenesis of human pancreatic islets. Cell Transplant 21: 1305-1320, 2012.
41. Barrientos S, Stojadinovic O, Golinko MS, Brem H and Tomic-Canic M: Growth factors and cytokines in wound healing. Wound Repair Regen 16: 585-601, 2008.
42. Zhang W, Bai X, Zhao B, Li Y, Zhang Y, Li Z, Wang X, Luo L, Han F, Zhang J, *et al*: Cell-free therapy based on adipose tissue stem cell-derived exosomes promotes wound healing via the PI3K/Akt signaling pathway. Exp Cell Res 370: 333-342, 2018.
43. Kutikhin AG, Sinitsky MY, Yuzhalin AE and Velikanova EA: Shear stress: An essential driver of endothelial progenitor cells. J Mol Cell Cardiol 118: 46-69, 2018.
44. Kumar VV, Heller M, Götz H, Schiegnitz E, Al-Nawas B and Kämmerer PW: Comparison of growth & function of endothelial progenitor cells cultured on deproteinized bovine bone modified with covalently bound fibronectin and bound vascular endothelial growth factor. Clin Oral Implants Res 28: 543-550, 2017.
45. Liang S, Wang Y and Liu Y: Dexmedetomidine alleviates lung ischemia-reperfusion injury in rats by activating PI3K/Akt pathway. Eur Rev Med Pharmacol Sci 23: 370-377, 2019.
46. Jin Z, Guo P, Li X, Ke J, Wang Y and Wu H: Neuroprotective effects of irisin against cerebral ischemia/reperfusion injury via Notch signaling pathway. Biomed Pharmacother 120: 109452, 2019.
47. Yang M, Kong DY and Chen JC: Inhibition of miR-148b ameliorates myocardial ischemia/reperfusion injury via regulation of Wnt/β-catenin signaling pathway. J Cell Physiol 234: 17757-17766, 2019.
48. Kahn M: Wnt signaling in stem cells and cancer stem cells: A tale of two coactivators. Prog Mol Biol Transl Sci 153: 209-244, 2018.
49. Oh SH, Kim HN, Park HJ, Shin JY and Lee PH: Mesenchymal stem cells increase hippocampal neurogenesis and neuronal differentiation by enhancing the Wnt signaling pathway in an Alzheimer's disease model. Cell Transplant 24: 1097-1109, 2015.
50. Chen S, Sun YY, Zhang ZX, Li YH, Xu ZM and Fu WN: Transcriptional suppression of microRNA-27a contributes to laryngeal cancer differentiation via GSK-3β-involved Wnt/β-catenin pathway. Oncotarget 8: 14708-14718, 2017.
51. Zhang X, Liu Y, Shao R and Li W: Cdc42-interacting protein 4 silencing relieves pulmonary fibrosis in STZ-induced diabetic mice via the Wnt/GSK-3β/β-catenin pathway. Exp Cell Res 359: 284-290, 2017.
52. Lin J, Song T, Li C and Mao W: GSK-3β in DNA repair, apoptosis, and resistance of chemotherapy, radiotherapy of cancer. Biochim Biophys Acta Mol Cell Res 1867: 118659, 2020.
53. Liao S, Wu J, Liu R, Wang S, Luo J, Yang Y, Qin Y, Li T, Zheng X, Song J, *et al*: A novel compound DBZ ameliorates neuroinflammation in LPS-stimulated microglia and ischemic stroke rats: Role of Akt(Ser473)/GSK3β(Ser9)-mediated Nrf2 activation. Redox Biol 36: 101644, 2020.
54. Xu B, Xu J, Cai N, Li M, Liu L, Qin Y, Li X and Wang H: Roflumilast prevents ischemic stroke-induced neuronal damage by restricting GSK3β-mediated oxidative stress and IRE1α/TRAF2/JNK pathway. Free Radic Biol Med 163: 281-296, 2021.
55. Zhou W, Yuan Y, Li J, Yuan WM, Huang LG and Zheng SW: Effect of Bifidobacterium on the mRNA expression levels of TRAF6, GSK-3β, and microRNA-146a in LPS-stimulated rat intestinal epithelial cells. Genet Mol Res 14: 10050-10056, 2015.
56. Duan J, Cui J, Yang Z, Guo C, Cao J, Xi M, Weng Y, Yin Y, Wang Y, Wei G, *et al*: Neuroprotective effect of Apelin 13 on ischemic stroke by activating AMPK/GSK-3β/Nrf2 signaling. J Neuroinflammation 16: 24, 2019.
57. Virgintino D, Errede M, Robertson D, Girolamo F, Masciandaro A and Bertossi M: VEGF expression is developmentally regulated during human brain angiogenesis. Histochem Cell Biol 119: 227-232, 2003.
58. Kim HG, Hwang YP and Jeong HG: Metallothionein-III induces HIF-1alpha-mediated VEGF expression in brain endothelial cells. Biochem Biophys Res Commun 369: 666-671, 2008.
59. Takano S, Uchida K, Inoue G, Matsumoto T, Aikawa J, Iwase D, Mukai M, Miyagi M and Takaso M: Vascular endothelial growth factor expression and their action in the synovial membranes of patients with painful knee osteoarthritis. BMC Musculoskelet Disord 19: 204, 2018.
60. Zhuang H, Shi S, Yuan Z and Chang JY: Bevacizumab treatment for radiation brain necrosis: Mechanism, efficacy and issues. Mol Cancer 18: 21, 2019.
61. Kubo H, Hayashi T, Ago K, Ago M, Kanekura T and Ogata M: Temporal expression of wound healing-related genes in skin burn injury. Leg Med (Tokyo) 16: 8-13, 2014.
62. Elbialy ZI, Atiba A, Abdelnaby A, Al-Hawary II, Elsheshtawy A, El-Serehy HA, Abdel-Daim MM, Fadl SE and Assar DH: Collagen extract obtained from Nile tilapia (Oreochromis niloticus L.) skin accelerates wound healing in rat model via up regulating VEGF, bFGF, and α-SMA genes expression. BMC Vet Res 16: 352, 2020.
63. Oryan A, Alemzadeh E and Eskandari MH: Kefir accelerates burn wound healing through inducing fibroblast cell migration in vitro and modulating the expression of IL-1ß, TGF-ß1, and bFGF genes in vivo. Probiotics Antimicrob Proteins 11: 874-886, 2019.
64. Zou Q, Wang W, Li Q, Liu J, Xu T and Zhao X: Effect of ultrasound debridement on serum inflammatory factors and bFGF, EGF expression in wound tissues. J Coll Physicians Surg Pak 29: 222-225, 2019.
65. Dykes IM and Emanueli C: Transcriptional and post-transcriptional gene regulation by long non-coding RNA. Genomics Proteomics Bioinformatics 15: 177-186, 2017.
66. Ariel F, Lucero L, Christ A, Mammarella MF, Jegu T, Veluchamy A, Mariappan K, Latrasse D, Blein T, Liu C, *et al*: R-loop mediated trans action of the APOLO long noncoding RNA. Mol Cell 77: 1055-1065.e4, 2020.